Abstract

To understand deep groundwater flow systems and their interaction with CO_2 emanated from magma at depth in a volcanic edifice, deep groundwater samples were collected from hot spring wells in the Aso volcanic area for hydrogen, oxygen and carbon isotope analyses and measurements of the stable carbon isotope ratios and concentrations of dissolved inorganic carbon (DIC). Relations between the stable carbon isotope ratio ($\delta^{13}C_{DIC}$) and DIC concentrations of the sampled waters show that magma-derived CO_2 mixed into the deep groundwater. Furthermore, groundwaters of deeper areas, except samples from fumarolic areas, show higher $\delta^{13}C_{DIC}$ values. The waters' stable hydrogen and oxygen isotope ratios (δD and $\delta^{18}O$) reflect the meteoric-water origin of that region's deep groundwater. A negative correlation was found between the altitude of the well bottom and the altitude of groundwater recharge as calculated using the equation of the recharge water line and δD value. This applies especially in the Aso-dani area, where deeper groundwater correlates with higher recharge. Groundwater recharged at high altitude has higher $\delta^{13}C_{DIC}$ of than groundwater recharged at low altitude, strongly suggesting that magmatic CO_2 is present to a much greater degree in deeper groundwater. These results indicate that magmatic CO_2 mixes into deeper groundwater flowing nearer the magma conduit or chamber.

Keywords:

Groundwater flow, magmatic CO_2, Disolved inorganic carbon, Stable isotope, Aso volcano,

Title

Mixing of magmatic CO_2 into volcano groundwater flow at Aso volcano assessed combining carbon and water stable isotopes

Authors

Makoto YAMADA, Shinji OHSAWA, Kohei KAZAHAYA, Masaya YASUHARA, Hiroshi TAKAHASHI, Kazuhiro AMITA, Hideo MAWATARI and Shin YOSHIKAWA

Affiliations

M. Yamada (Corresponding author), S. Ohsawa, H. Mawatari

Beppu Geothermal Research Laboratory, Institute for Geothermal Sciences, Graduate School of Science, Kyoto University, Noguchibaru, Beppu, Oita, Japan

K. Kazahaya, M. Yasuhara, H. Takahashi

Research Center for Deep Geological Environments, Geological Survey of Japan, National Institute of Advanced Industrial Science and Technology, Tsukuba, Japan

K. Amita

Department of Earth Science and Technology, Faculty of Engineering and Resource Science, Akita University, Akita, Japan

S. Yoshikawa

Aso Volcanological Laboratory, Institute for Geothermal Sciences, Graduate School of Science, Kyoto University, Aso, Kumamoto, Japan

Total text pages: 20

Numbers of table and figures: 9

Address for Proofs:

Makoto Yamada

Institute for Geothermal Sciences, Graduate School of Science, Kyoto University, Noguchibaru, Beppu 874-0903, Oita, Japan

Tel.: +81-977-22-0713 Fax: +81-977-22-0965

e-mail: yamada@bep.vgs.kyoto-u.ac.jp

1. Introduction

Stable carbon isotope studies of groundwater systems at some volcanoes have revealed that deeply derived CO_2 mixes into groundwater that contains CO_2 derived from soils (Chiodini et al., 2000; Ohsawa et al., 2002; Evans et al., 2002; Caliro et al., 2005). These studies, using datasets of stable carbon isotope ratios and concentrations of dissolved inorganic carbon (DIC), present a robust approaches to determine whether or not magmatic CO_2 is dissolved by groundwater. In addition, it is possible to determine recharge elevations of groundwaters using stable hydrogen and oxygen isotopes based on isotopic altitude effects of precipitation (Yasuhara et al., 1993; Kazahaya et al., 1999; Nakamura et al., 2002; Yasuhara et al., 2002). Using this technique, it is possible to investigate groundwater movement in volcanic edifices. Both of these isotopic methods are powerful tools for investigating the groundwater hydrology of volcanoes.

It is expected that the combined use of these two methods, as first demonstrated at Kuju volcano by Yamada et al. (2005), will be effective to deepen our understanding of the input of magmatic CO_2 into volcano groundwater flow systems. Although Yamada et al. (2005) studied shallow groundwater flow systems forming cold carbonic springs and bicarbonate-type hot spring, deep groundwater flow systems and their interaction with CO_2 from deep-seated magma requires analysis of groundwater from deep wells drilled into the volcanic edifice. As new hot springs for bathing have been developed by deep drilling in Japan, including at Aso volcano, we have investigated the interaction between magmata CO_2 and deep groundwater using hot spring wells at Aso volcano.

In this paper, we first present results of the isotope and DIC analyses of hot spring waters, and then assess these results to determine the importance of magmatic CO_2 in deep groundwater in the vicinity of Aso volcano. Results suggest a latent mixing process of magmatic CO_2 into the deep groundwater flow system at Aso volcano.

2. Site description and Methods

Aso volcano is an active volcano in Kyushu Island, southwest Japan. This volcano is characterized by a large caldera, extending 18 km east-west and 25 km north-south, where a central cone is located (Fig. 1). The caldera floor is divided into north and south parts called Aso-dani (Aso Valley) and Nango-dani (Nango Valley) respectively. As Aso-dani is covered with lake sediment (Tanaka, 2000), the Aso-dani landform is much flatter than that of Nango-dani, implying a simple stratified structure of the groundwater flow system at the Aso-dani area. Two large rivers, called Kurokawa and Shirakawa, respectively flow on the lowest part of caldera floors at Aso-dani and Nango-dani. Those rivers, which meet within the caldera, flow out from the caldera at the western rim of the caldera.

Surface geothermal activities of Aso volcano are only observed on the central cones. One type of activity is characterized by volcanic gas discharge from a hot, highly acidic crater lake at the first crater of Mt. Naka-dake (e.g. Saito et al., 2008); the other is characterized by fumarolic gas discharges originated from hydrothermal systems at Yuno-tani and Tarutama areas on the western slope of Mt. Eboshi-dake (NEDO, 1989) (Fig. 1). Many natural hot springs in and around those areas are recognized as steam-heated hot springs and have been used from antiquity. Recently, many “hot springs” aside from those in the Uchinomaki area (AHL02–AHL05 in Fig. 1) have been developed for bathing by drilling to about 1000 m deep. Although proprietary chemical data of major dissolved constituents of hot spring waters from *Onsen-bunsekisho* (data tables of hot springs' water quality that must be kept by Japanese law), formation processes of the hot spring waters, including their relation to magmatic emanation, have not been investigated at Aso volcano.

Hot spring water samples from 23 wells of variable depth were collected to produce datasets of concentrations and stable carbon isotope compositions of dissolved inorganic carbon (DIC and $\delta^{13}C$, respectively), stable isotopic composition of water (δD and $\delta^{18}O$) and of concentrations major ions (Na, K, Mg, Ca, Cl, SO_4 and HCO_3). Cold spring waters were also collected to determine the relation between δD and recharge elevation of hot spring waters following the method described by Kazahaya and Yasuhara (1994). The samples for water isotope analysis were collected in a glass vial to avoid water evaporation. The samples collected in a CO_2 gas-tight bottle, were stored in a refrigerator at 5°C until chemical and isotopic analyses were undertaken. Water temperature and pH were measured in the field. All sampling locations are presented in Fig. 1.

Major ions (Na, K, Mg, Ca, Cl and SO_4) were determined by ion-chromatography (DX-120, Dionex) and HCO_3 by acid titration. The concentrations of DIC were determined using a CO_2-gas electrode (CE-2041; DKK–TOA Corp.) with an ion meter (IM-22P; DKK–TOA Corp.) after all the carbonate species in the sample water (9 ml) were converted into CO_2(aq) by the addition of 1 ml of 10% sulfuric acid. The water samples for measurement of δ^{13}C were injected into a glass vial containing phosphoric acid and filled with helium gas. The generated CO_2 gas in the vial was transferred to a mass spectrometer (Delta-Plus; Thermo Finnigan) through pre-treatment equipment of carbon stable isotope of DIC (Gas Bench II; Thermo Finnigan). The obtained δ^{13}C is shown using δ notation as ‰-deviation from the value of Vienna-Peedee Belemnite (V-PDB). The oxygen and the hydrogen isotope ratios (δD and δ^{18}O) of the water samples were determined using a mass spectrometer (Geo 20-20 model installed at the Stable Isotope Laboratory of IGNS, New Zealand) with the zinc reduction method and CO_2 equilibration method. The obtained δD and δ^{18}O are shown using δ notation as ‰-deviation from the value of SMOW. The analytical precisions are ±0.5mg/l for major ions, ±0.3mmol/l for DIC, ±0.2‰ for δ^{13}C, ±1.0‰ for δD and ±0.1‰ for δ^{18}O, respectively. All analytical results are presented in Table 1.

3. Results and Discussion

3.1. Dissolved inorganic carbon

The relationship between $\delta^{13}C$ and DIC are shown in Fig. 2. The two lines in Fig. 2 show theoretical mixing curves calculated considering the dissolution of magmatic CO_2 by a groundwater which initially contained only biogenic soil CO_2. Although the actual mixing process could be more complex, we estimated the simple theoretical mixing curves because the influence of the isotopic fractionation is so small that we can neglect it because of the following reasons: (1) the all saturation indexes for the calcite were less than 1 (Table 1; SI is calculated by use of the chemical and physical data of the water), implying no precipitation of calcite, or precipitation at a very low rate when the saturation index exceeds the value of 1 (Dandurand et al., 1982; Alessandro et al., 2007): (2) we were careful to sample waters degassing. The equation used to compute these theoretical curves is the following:

$$\delta^{13} C_g = \frac{C_0 \times (\delta^{13} C_0 - \delta^{13} C_{in})}{C_g} + \delta^{13} C_{in} \qquad (1)$$

where C_0 and C_g represent DIC concentrations of the initial value and the value after mixing respectively, and where $\delta^{13}C_0$, $\delta^{13}C_{in}$, and $\delta^{13}C_g$ denote the stable carbon isotope ratio of the initial value, the value of input gas, and the value after mixing respectively. Here, the $\delta^{13}C$ value of a fumarolic CO_2 discharged from Tarutama area (-5‰ ; NEDO, 1989) was used for $\delta^{13}C_{in}$ as magmatic gas, and for $\delta^{13}C_0$ and C_0 consistent with groundwater values in equilibrium with soil CO_2, (-30‰, 0.1 mmol/L) and (-30‰, 1 mmol/L) were used. The -30‰ is the lowest value of cold spring water in this area (CS01). Almost all data points are shown on these mixing lines or the enclosed area between the two lines. Ohsawa et al. (2002) suggested using the same kind of $\delta^{13}C_{DIC}$ versus DIC concentration diagram that magmatic CO_2 mixes into soil CO_2 dissolved groundwaters having variable DIC concentrations in Unzen volcano, Japan. Chiodini et al. (2000) presented a similar interpretation using a $\delta^{13}C_{DIC}$ versus DIC diagram for central Apennine Italy. Consequently, the results obtained in this study demonstrate that all hot spring waters in Aso volcano are contaminated by magmatic CO_2 to varying degrees.

The mixing relation showed on Fig. 2 provides an effective index for expressing the degree of magmatic CO_2 mixing because $\delta^{13}C_{DIC}$ value increases with the amounts of mixed magmatic CO_2. In other words, $\delta^{13}C_{DIC}$ of hot spring water will be higher if it is contaminated by more magmatic CO_2. Figure 3 presents relations between $\delta^{13}C_{DIC}$ of hot spring waters and altitudes of hot spring well bottoms, for the Aso-dani area (A), the Nango-dani area (B), and the whole area (C). The data plot of Aso-dani area (Fig. 3A) portrays a clear increase in $\delta^{13}C_{DIC}$ value with decreasing altitude of the well bottom, although the data plots of Nango-dani area (Fig. 3B) show no such clear tendency. However, as depicted in Fig. 3C, some plots of the Nango-dani area agree in the tendency of that of Aso-dani area. This tendency suggests a groundwater system forming in which more magmatic CO_2 mixes in the deeper groundwater (Fig. 3C). Five samples, hatched in fig 3c. (NHC01, NHC02, NHC06, NHL02, and NHL04 in Fig. 1), show a different behavior. With the exception of NHL02, topographic catchment areas of these hot spring waters include Yunotani and Tarutama fumarolic areas. As described above, these areas are active geothermal areas with fumarolic gas discharges and natural hot springs of steam-heated type. The fumarolic gases in these areas include a magmatic gas component (Ohsawa et al., 1997). It can therefore be inferred that magmatic CO_2 rises near the surface around these areas. Hence hot spring waters that do not show the typical correlation between $\delta^{13}C$ and the altitude of the well bottom, as described above, are produced by near surface mixing of ascending magmatic CO_2 and shallow groundwater. This “exceptional” mixing process is linked with the well known formation mechanism of volcanic hot spring water of bicarbonate type. This study has shed light on a formation mechanism of hot spring water in the volcanic edifice different from well known processes. Regarding the formation process of the NHL02 hot spring water, we cannot reach a definite answer because of insufficient data.

3.2. Water isotopes

The δD and $\delta^{18}O$ values of groundwater samples vary from -62.2‰ to -44.2‰ and -9.2‰ to -7.2‰, respectively. Results are shown on the δD versus $\delta^{18}O$ diagram with the field of andesitic magmatic steam (Giggenbach, 1992) and the meteoric water line ($\delta D = 8\delta^{18}O + 10$: Craig, 1961) (Fig. 4). All data of groundwater samples are lie along the meteoric water line, indicating that hot spring waters are derived almost entirely from meteoric water, and that magmatic steam does not mix with groundwater.

In the case where groundwater originates from meteoric water, the recharge altitude of that groundwater can be estimated using the recharge water line: a relation between δD values and mean recharge altitude in the studied area (e.g., Yasuhara et al., 1993; Kazahaya and Yasuhara, 1994; Nakamura et al., 2002; Yasuhara et al., 2002). In this study, four cold spring water samples (CS01–CS04) were used to determine the local recharge-water line. The recharge-water line of Aso volcano is determined as $H = -56.4 \delta D - 2063$, where H expresses the recharge altitude. The obtained relation is presented in Fig. 5. The vertical bars associated with data points show the topographic recharge altitude of each cold spring.

The relation between the δD data of hot spring waters and altitudes of hot spring well bottoms is presented in Fig. 5. A slight positive tendency of the relation is apparent, which suggests that hot spring water recharged at high altitude flows deeper than that at low altitude. To clarifying this, we examined the relation between the altitudes of well bottoms and the recharge altitudes of hot spring waters, dividing them into four groups according to their location: central cones at Aso-dani side, central cones at Nago-dani side, Aso-dani to caldera rim, and Nango-dani to caldera rim. As depicted in Fig. 6, negative correlations were found between the altitudes of well bottoms and the recharge altitudes of hot spring waters in every area, although correlation levels differed among areas. Furthermore, it can be inferred from the correlation line's slopes that the groundwater flow systems forming hot spring waters in Aso-dani areas (central cones at Aso-dani side and Asodani to caldera rim) are more strongly layered than those in Nango-dani areas (central cones at Nago-dani side and Nango-dani to caldera rim). The systematic relations of recharge altitude and flow depth of hot spring waters in Aso-dani areas are consistent with the general conceptualization of deep groundwater flow systems (Ward and Robinson, 1990): the higher elevation at which the groundwater is recharged, the deeper the groundwater flows. In contrast, in Nango-dani areas, the deep groundwaters that are recharged at several altitudes tend to come together into an almost identical aquifer.

4. Conclusions

In section 3.1 we have shown that at Aso volcano, deeper groundwater has a stronger interaction with magmatic CO_2, except in the vicinity of the Yunotani and Tarutama areas. On the other hand, in section 3.2, it was shown that deeper groundwater was recharged at higher altitude. This relation is evident in Aso-dani areas of the northern part of Aso caldera, which is not inconsistent with the groundwater circulation in the stratified volcanic deposits (see section 2.). Combining the results obtained from the inspection of carbon and water isotopes are evident that the $\delta^{13}C_{DIC}$ of groundwater recharged at high altitude is more positive than that at low altitude (Fig. 7). Figure 7 presents the good relations between recharge altitude and flow depth of hot spring waters for the Aso-dani areas (central cones at Aso-dani side and Asodani to caldera rim). As clearly shown in Fig. 7, the $\delta^{13}C_{DIC}$ of groundwater recharged at high altitude is more positive than that infiltrating at low altitude, suggesting a significant contribution of magmatic CO_2 for such deeper groundwater.

From a simple geometrical consideration of a layered groundwater flow system in volcanic edifice, it is readily understood that groundwater recharged at the highest altitude flows much nearer the magma conduit or chamber than those recharged at low altitudes (Fig. 8). Consequently, the much deeper groundwaters in Aso-dani areas are thought to be affected strongly by mixing of magmatic CO_2. For that reason, results of our study suggest that magmatic CO_2 was mixed into the volcano groundwater flow system at Aso volcano. This mechanism differs from the well known mixing process on the formation of bicarbonate type hot spring waters observed in the vicinity of the Yunotani and Tarutama areas (see section 3.1.).

It is reasonable to believe that deep groundwaters are influenced by the magmatic emanation at the central cone side of Aso-dani area, although it is not easy to understand why such a system is apparent at Uchinomaki area at the northern end of Asodani to the caldera rim far from the central cones (AHL02–AHL05 in Fig. 1). For clarification of this point, further geophysical explorations in and around the central cones (e.g., Tsutsui and Sudo, 2004; Hase et al., 2005; Kanda et al., 2008) are necessary.

Acknowledgements

We thank G. Lyon, K. Rogers, and W. Gooley for assistance with hydrogen and oxygen isotope analyses. This research was partially supported by the Ministry of Education, Science, Sports and Culture, Grant-in-Aid for Scientific Research (B), 19310116. Anonymous referees provided useful comments that led to considerable improvements in this manuscript.

References

Alessandro, W.D., Giammanco, S., Bellomo, S. and Parello, F., 2007. Geochemistry and mineralogy of travertine deposits of the SW flank of Mt. Etna (Italy): Relationships with past volcanic and degassing activity. J Volcanol Geotherm Res 165, 64–70.

Caliro, S., Chiodini, G., Avino, R., Cardellini, C. and Frondini, F., 2005. Volcanic degassing at Somma-Vesuvio (Italy) inferred by chemical and isotopic signatures of groundwater. Appl. Geochem., 20, 1060-1076.

Chiodini, G., Frondini, F., Cardellini, C., Parello, F. and Peruzzi, L., 2000. Rate of diffuse carbon dioxide Earth degassing estimated from carbon balance of regional aquifers: The case of central Apennine, Italy. J Geophys Res 105, 8423–8434.

Craig, H., 1961. Isotopic variations in meteoric waters. Science 133, 1833–1834.

Dandurand, J.L., Gout, R., Hoefs, J., Menschel, G., Schott, J. and Usdowski, E., 1982. Keinetically controlled variations of major components and carbon and oxygen isotopes in a calcite-precipitating spring. Chemical Geotlogy 36, 299–315.

Evans, W.C., Sorey, M.L., Cook, A.C., Kennedy, B.M., Shuster, D.L., Colvard, E.M., White, L.D. and Huebner, M.A., 2002. Tracing and quantifying magmatic carbon discharge in cold ground waters: lessons learned from Mammoth Mountain, USA. J Volcanol Geotherm Res 114, 291–312.

Giggenbach, W.F., 1992. Isotopic shifts in waters from geothermal and volcanic system along convergent plate boundaries and their origin. Earth Planet Sci Lett 113, 495–510.

Hasea, H., Hashimoto, T., Sakanaka, S., Kanda, W. and Tanaka, Y., 2005. Hydrothermal system beneath Aso volcano as inferred from self-potential mapping and resistivity structure. J Volcanol Geotherm Res 143, 259–277.

Kanda, W., Tanaka, Y., Utsugi, M., Takakura, S., Hashimoto, T. and Inoue, H., 2008. A preparation zone for volcanic explosions beneath Naka-dake crater, Aso volcano, as inferred from magnetotelluric surveys. Journal Volcanol Geotherm Res 178, 32–45.

Kazahaya, K. and Yasuhara, M., 1994. A hydrogen isotopic study of spring in Mt.

Yatsugatake, Japan: Application to groundwater recharge and flow processes. J Japanese Association of Hydrol Sci 24, 107–119. (in Japanese)

Kazahaya, K. and Yasuhara, M., 1999. Groundwater movement in Iwate volcano: preconsideration result for isotope-hydrological study. Chikyu Monthly 21, 290–295. (in Japanese)

Nakamura, T., Sato, T. and Yasuhara, M., 2002. Isotopic altitude effects of meteoric water in the southeastern slope of Mt. Ontake, Japan. J Japanese Association of Hydrol Sci 32, 135–147. (in Japanese)

New Energy Development Organization (NEDO), 1989. Regional exploration of geothermal fluid circulation system, Aso area, National Geothermal Resources Exploration Project (3rd phase). NEDO, Japan. (in Japanese)

Ohsawa, S., Yusa, Y., Oue, K. and Kitaoka, K., 1997. Inert gas compositions of fumarolic gases discharged from the Aso volcanic-geothermal region, Japan. J Balneol Soc Japan 47, 56–67. (in Japanese)

Ohsawa, S., Kazahaya, K., Yasuhara, M., Kono, T., Kitaoka, K., Yusa, Y. and Yamaguchi, K., 2002. Escape of volcanic gas into shallow groundwater systems at Unzen Volcano (Japan): Evidence from chemical and stable carbon isotope compositions of dissolved inorganic carbon. Limnology 3, 169–173.

Saito, T., Ohsawa, S., Hashimoto, T., Terada, A., Yoshikawa, S. and Ohkura, T., 2008. Water, heat and chloride balances of the crater lake at Aso volcano, Japan. J Geotherm Res Soc Jpn 30, 107–120. (in Japanese)

Tanaka, N., 2000. The history of Ichinomiya-cho, Mt. Aso and Water. Ichinomiya-cyo, Kumamoto Japan. (in Japanese)

Tsutsui, T. and Sudo, Y., 2004. Seismic reflectors beneath the central cones of Aso Volcano, Kyushu, Japan. Journal Volcanol Geotherm Res 131, 33–58.

Ward, R.C. and Robinson, M., 1990. Principles of Hydrology Third edition. McGraw-Hill, London.

Yamada, M., Amita, K. and Ohsawa, S., 2005. Isotope-hydrological Study on Formation Mechanism of Carbonate Springs at the Southeastern Foothills of Kuju Volcano, Central Kyushu, Japan. J Balneol Soc Japan 54, 163–172. (in Japanese)

Yasuhara, M., Marui, A. and Kazahaya, K., 1993. An isotopic study of groundwater flow in a volcano under humid climatic conditions. Tracers in Hydrology 215.179-186.

Yasuhara, M., Kazahaya, K., Inamura, A., Kono, T., Ohsawa, S., Yusa, Y., Kitaoka, K., Hoshizumi, H., Sumii, T. and Uto, K., 2002. Hydraulic construction of Unzen volcano. Chikyu Monthly 24, 849–857. (in Japanese)

Figure and Table legends

Figure 1

Map showing sampling locations at Aso volcano, Japan. Sampling points of hot springs are shown as diamond, triangle, square, and circle symbols, respectively, on the central cone side of Kurokawa River, caldera limb side of Kurokawa River, central cone side of Shirakawa River, and caldera limb side of Shirakawa River. Hexagonal symbols denote cold spring sampling sites.

Figure 2

Concentrations of dissolved inorganic carbon (DIC) versus $\delta^{13}C_{DIC}$. Two lines represent theoretical curves calculated by adding magmatic CO_2 to initial groundwater dissolved soil CO_2. For details, see the text.

Figure 3

Relation between $\delta^{13}C_{DIC}$ values and altitude of the well bottom of hot springs. (A), (B), and (C) respectively show data of the Aso-dani area, the Nango-dani area, and the whole area.

Figure 4

The δD-$\delta^{18}O$ plots of study-area groundwater. The diagonally shaded box shows ranges of δD and $\delta^{18}O$ values of andesitic magmatic steam (Giggenbach, 1992). The solid line expresses the meteoric water line: $\delta D = 8\ \delta^{18}O + 10$ (Craig, 1961).

Figure 5

The δD value versus altitude of the well bottom. The solid line shows the recharge-water line ($H = -56.4\delta D - 2063$, where H expresses the recharge elevation) as estimated using data of four cold springs.

Figure 6

Relations between the well bottom altitude and recharge altitude as calculated using the equation of recharge-water line and δD value. Regression lines and correlation factors are shown on each diagram.

Figure 7

Relation between $\delta^{13}C_{DIC}$ values and recharge altitude as calculated using the equation of recharge-water line and δD value in Aso-dani. Solid and broken lines respectively show the regression lines of the central cone side samples and caldera limb side samples.

Figure 8

Conceptual image of groundwater flow and inflow of magmatic CO_2 for groundwaters in Aso volcano at the Aso-dani central cone side. Magmatic CO_2 escaped from the magma conduit or chamber to volcanic edifice mixes into groundwater recharged at the high altitude area of the central volcanic cone and flowing through in the proximity of the magma conduit.

Figure 1

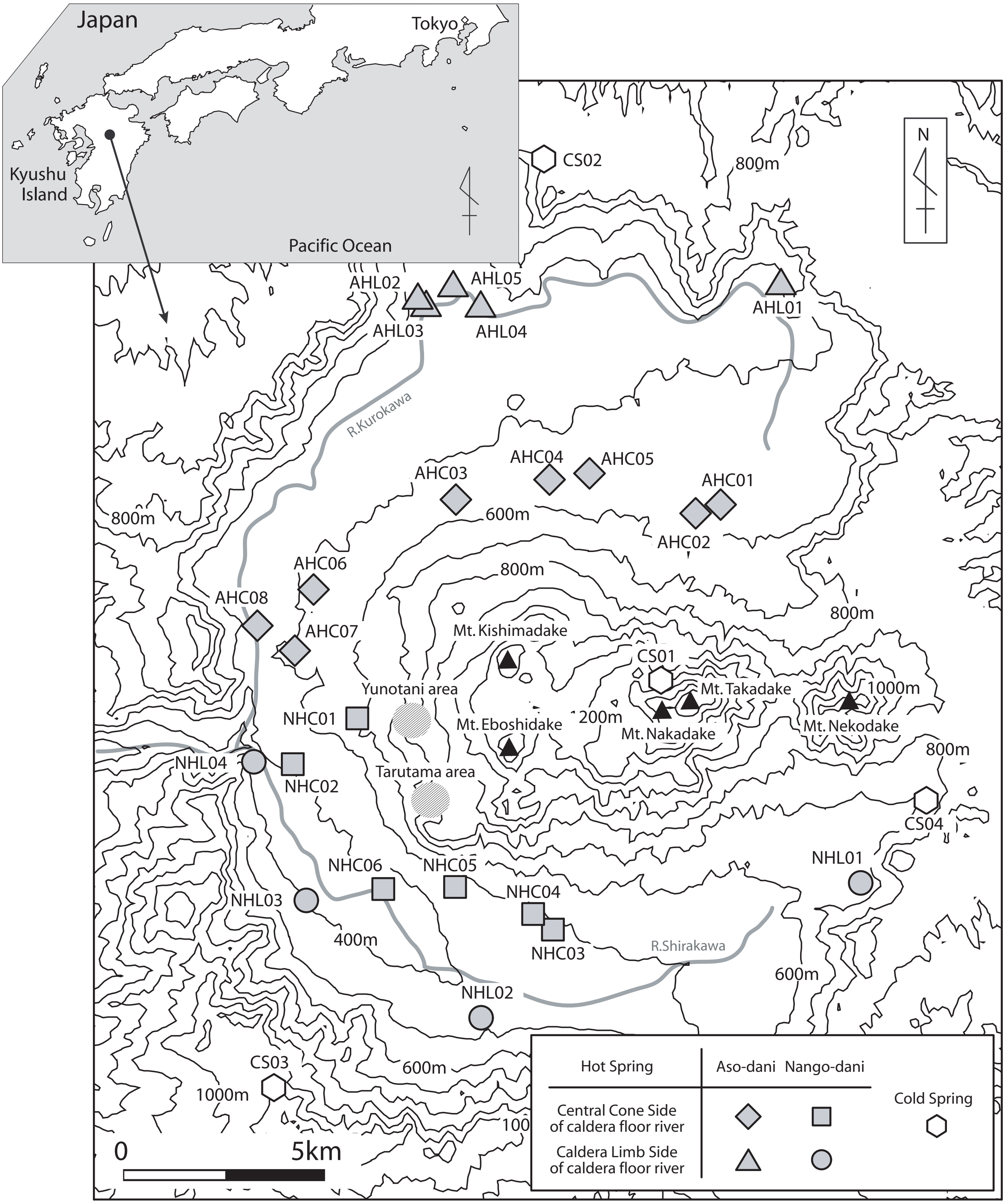

Japan
Tokyo
Kyushu Island
Pacific Ocean
N
CS02
800m
AHL02
AHL05
AHL01
AHL03
AHL04
R.Kurokawa
AHC04
AHC05
AHC03
AHC01
800m
600m
AHC02
AHC06
800m
AHC08
800m
AHC07
Mt. Kishimadake
CS01
Yunotani area
Mt. Takadake
1000m
NHC01
Mt. Eboshidake
200m
Mt. Nakadake
Mt. Nekodake
800m
NHL04
NHC02
Tarutama area
CS04
NHC06
NHC05
NHL01
NHL03
NHC04
400m
NHC03
R.Shirakawa
600m
NHL02
600m
CS03
1000m
100
0
5km
Hot Spring
Aso-dani
Nango-dani
Central Cone Side of caldera floor river
Caldera Limb Side of caldera floor river
Cold Spring

Figure 2

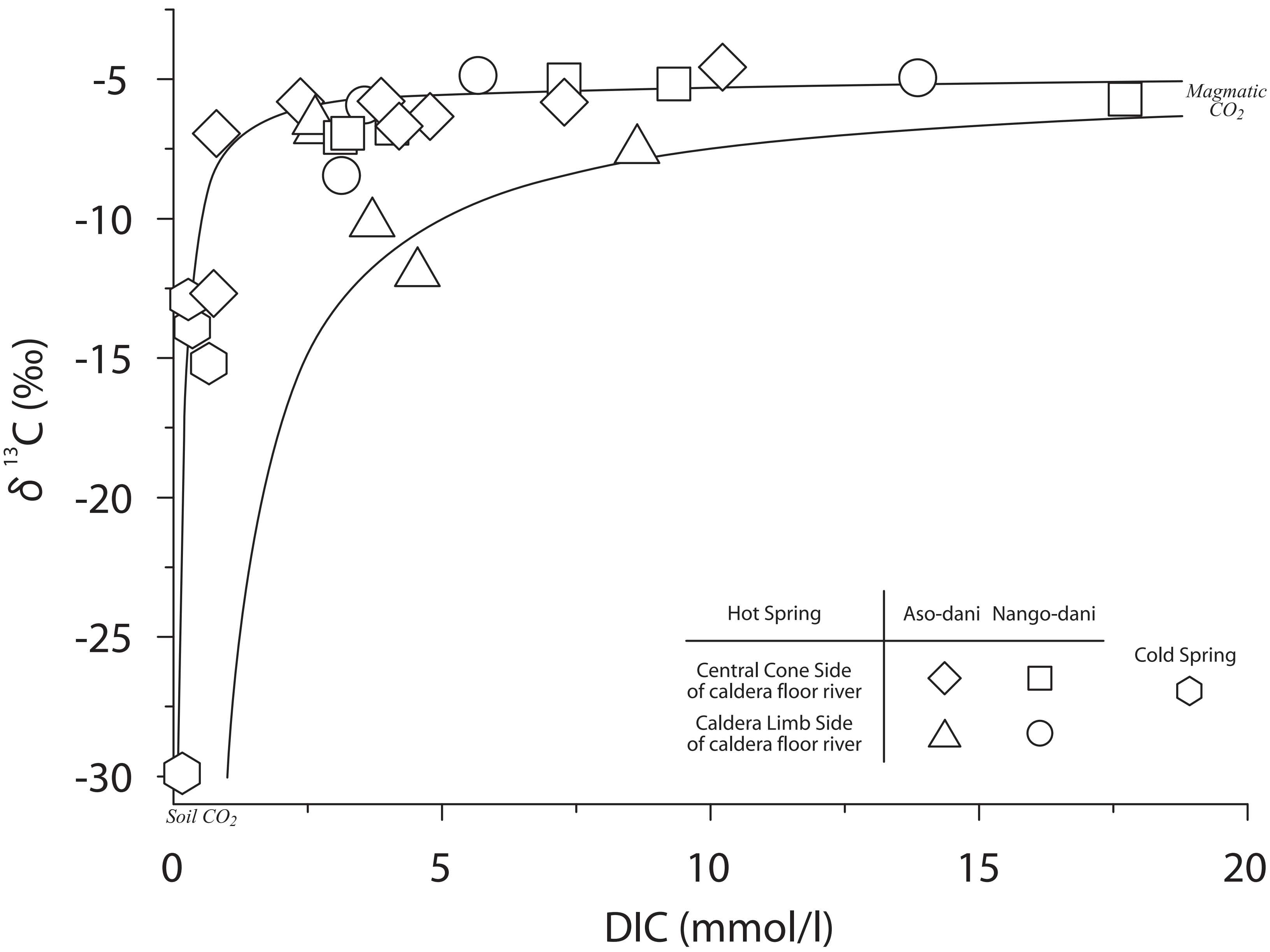

-5
-10
-15
-20
-25
-30
δ 13C (‰)
0
5
10
15
20
DIC (mmol/l)
Soil CO2
Magmatic CO2
Hot Spring
Aso-dani
Nango-dani
Central Cone Side of caldera floor river
Caldera Limb Side of caldera floor river
Cold Spring

Figure 3

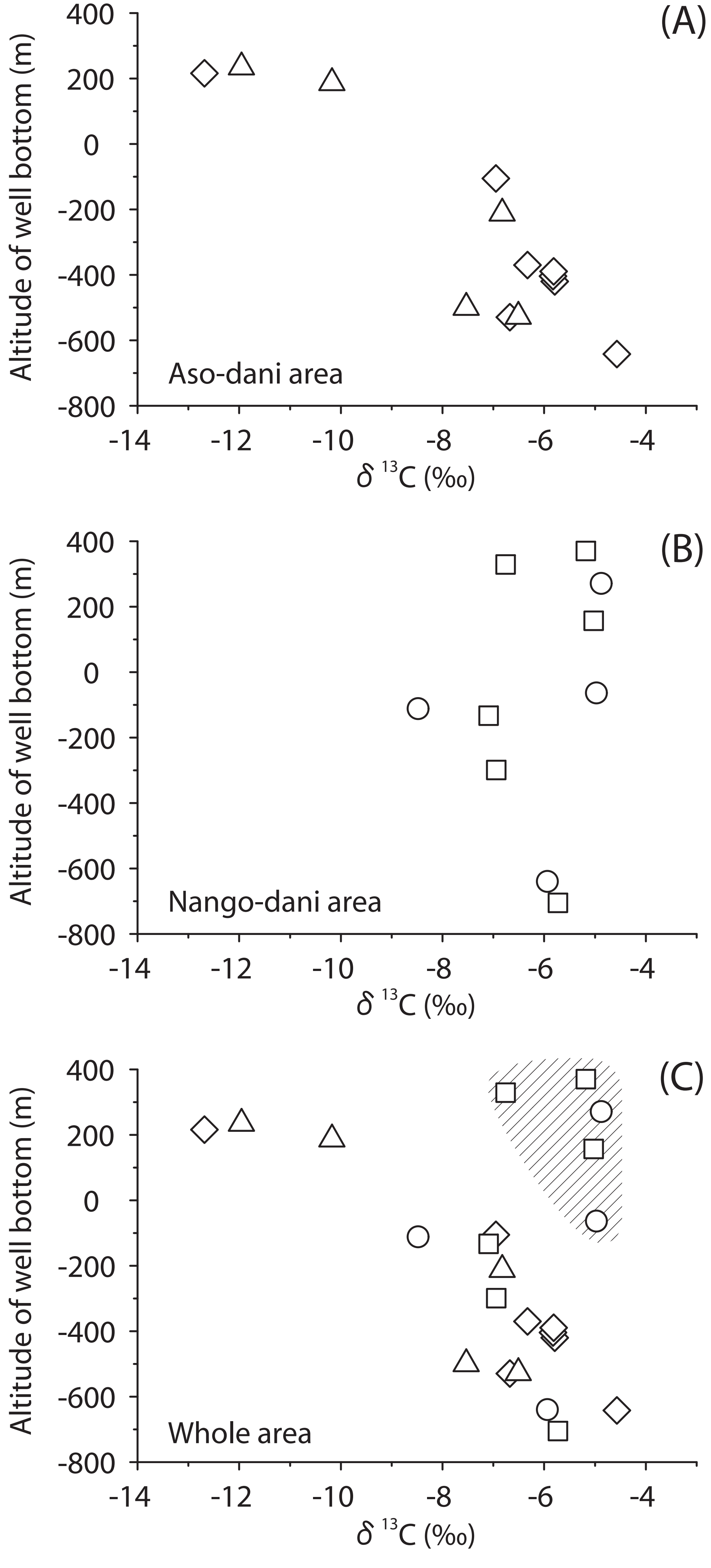
(A)
Aso-dani area
Altitude of well bottom (m)
400
200
0
-200
-400
-600
-800
-14
-12
-10
-8
-6
-4
δ 13C (‰)
(B)
Nango-dani area
Altitude of well bottom (m)
δ 13C (‰)
(C)
Whole area
Altitude of well bottom (m)
δ 13C (‰)

Figure 4

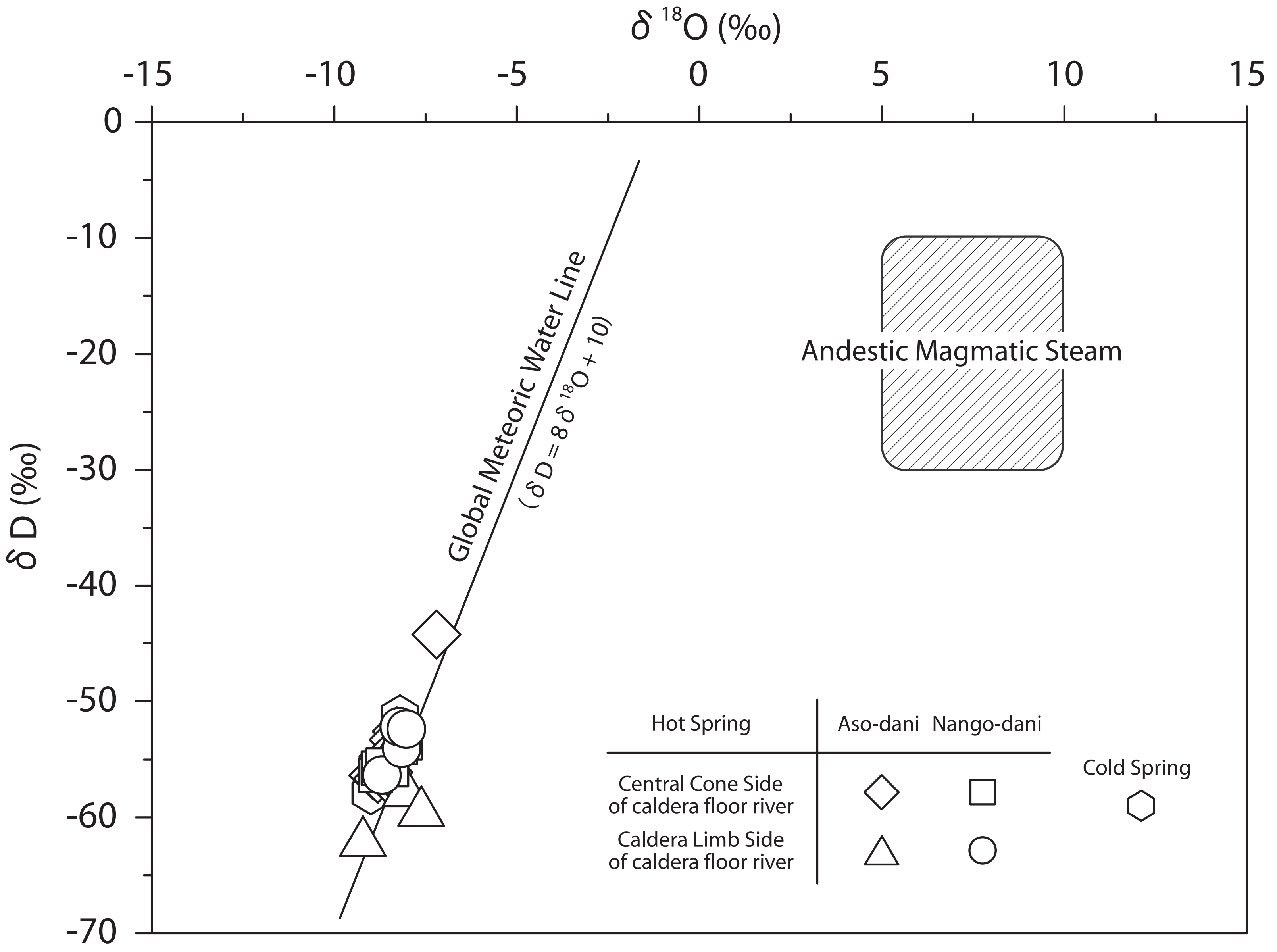
δ 18O (‰)
-15
-10
-5
0
5
10
15
0
-10
-20
-30
-40
-50
-60
-70
δ D (‰)
Global Meteoric Water Line
(δ D = 8 δ 18O + 10)
Andestic Magmatic Steam
Hot Spring
Aso-dani
Nango-dani
Central Cone Side
of caldera floor river
Caldera Limb Side
of caldera floor river
Cold Spring

Figure 5

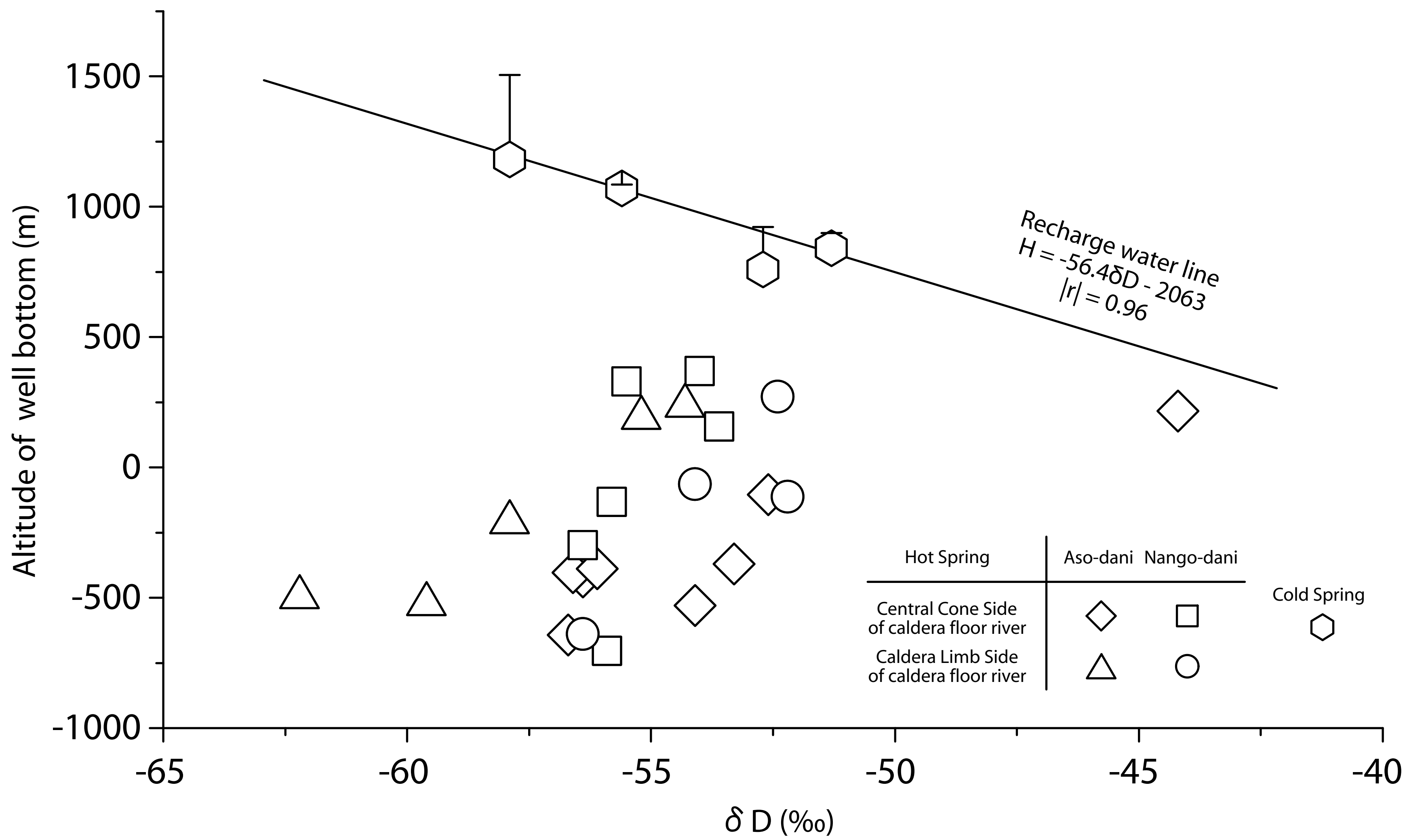

Recharge water line
H = -56.4δD - 2063
|r| = 0.96
Altitude of well bottom (m)
1500
1000
500
0
-500
-1000
-65
-60
-55
-50
-45
-40
δ D (‰)
Hot Spring
Aso-dani
Nango-dani
Central Cone Side of caldera floor river
Caldera Limb Side of caldera floor river
Cold Spring

Figure 6

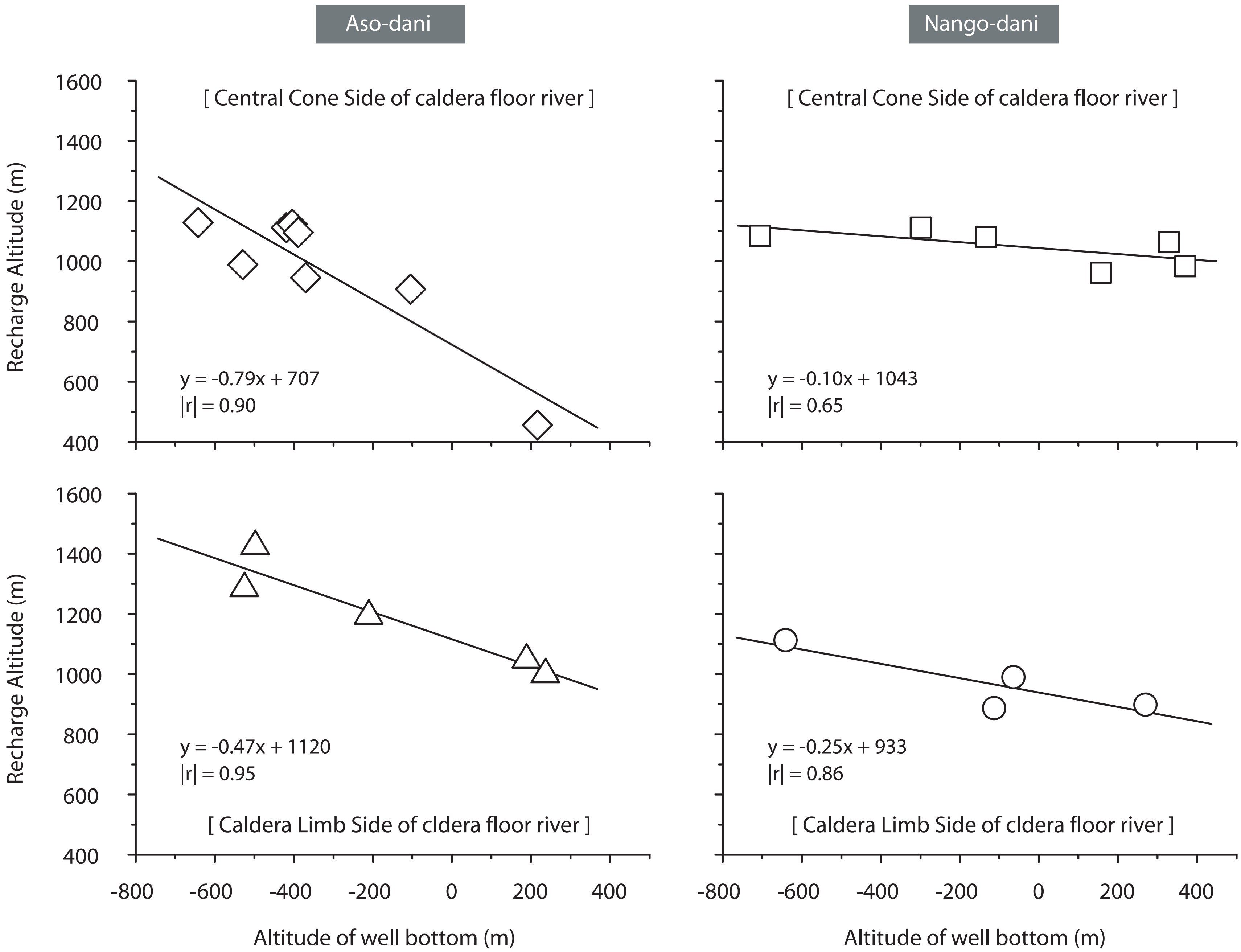

Aso-dani
Nango-dani
[Central Cone Side of caldera floor river]
[Central Cone Side of caldera floor river]
y = -0.79x + 707
|r| = 0.90
y = -0.10x + 1043
|r| = 0.65
y = -0.47x + 1120
|r| = 0.95
y = -0.25x + 933
|r| = 0.86
[Caldera Limb Side of cldera floor river]
[Caldera Limb Side of cldera floor river]
Recharge Altitude (m)
Recharge Altitude (m)
1600
1400
1200
1000
800
600
400
-800
-600
-400
-200
0
200
400
Altitude of well bottom (m)
Altitude of well bottom (m)

Figure 7

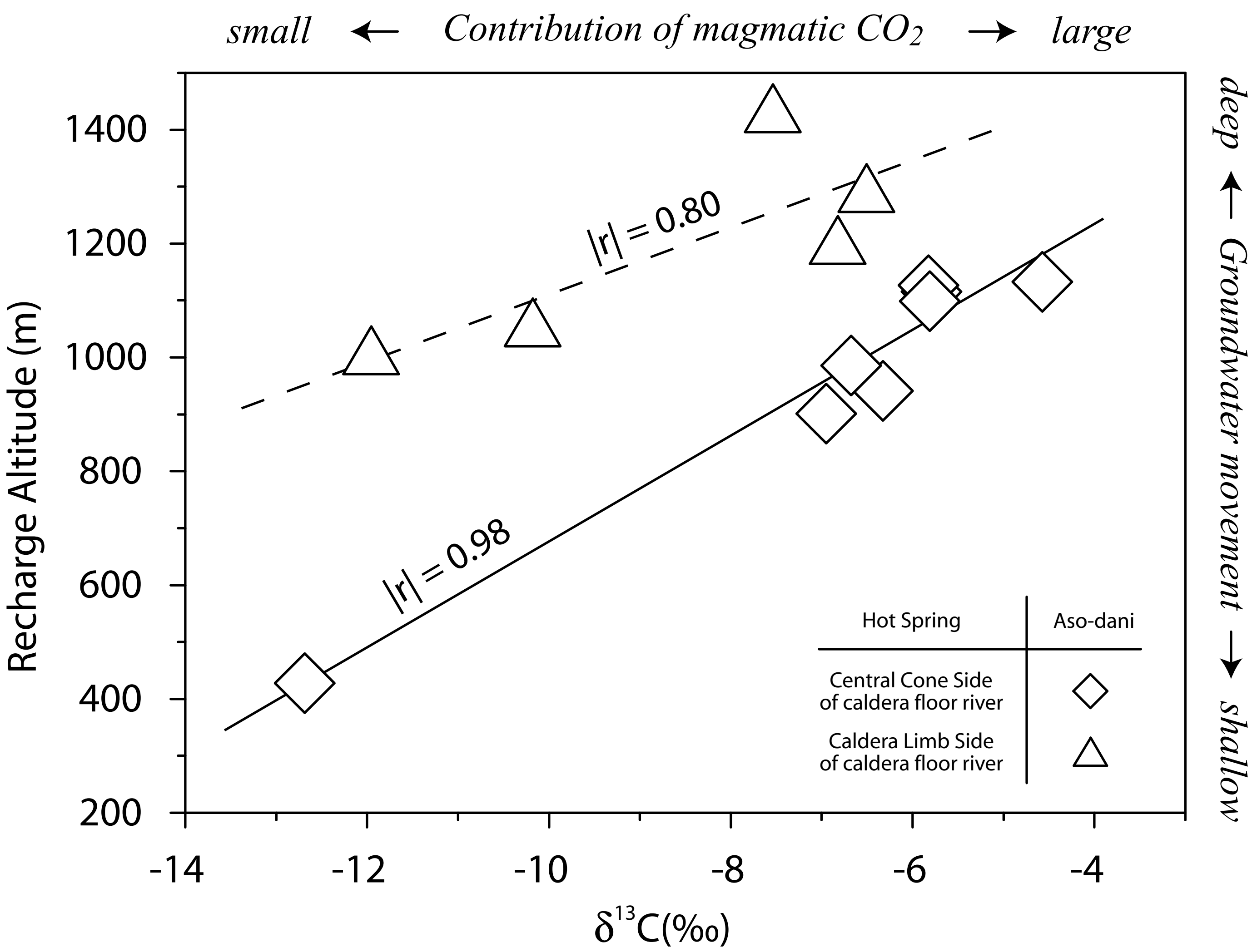

small ← Contribution of magmatic CO2 → large
deep ← Groundwater movement → shallow
Recharge Altitude (m)
1400
1200
1000
800
600
400
200
-14
-12
-10
-8
-6
-4
δ13C(‰)
|r| = 0.80
|r| = 0.98
Hot Spring
Aso-dani
Central Cone Side
of caldera floor river
Caldera Limb Side
of caldera floor river

Figure 8

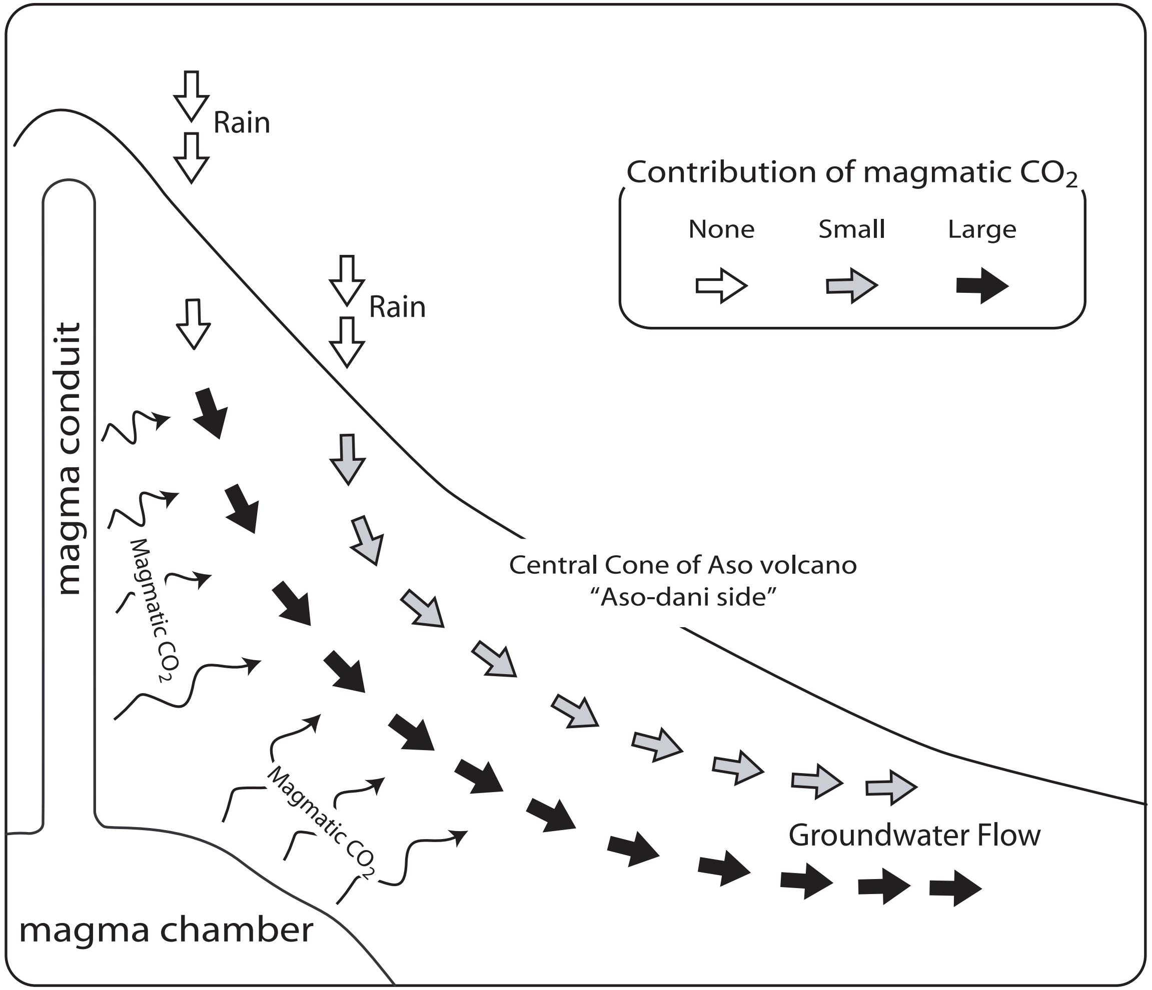
Rain
Rain
Contribution of magmatic CO_2
None
Small
Large
magma conduit
Magmatic CO_2
Magmatic CO_2
Central Cone of Aso volcano
"Aso-dani side"
Groundwater Flow
magma chamber